DOI: 10.1002/ejic.201000896

Solvent-Dependent *cis*/*trans* Isomerism at the Paddlewheel Mo_2 Core of Linear Tetranuclear Clusters of Mo^{II} and Cu^{I} Supported by 6-(Diphenylphosphanyl)-pyridin-2-olate (pyphos)

Kuntal Pal,[a] Keisuke Nakao,[a] and Kazushi Mashima*[a]

In memory of Professor Frank Albert Cotton

Keywords: Copper / Molybdenum / Cluster compounds / Multinuclear clusters / Solvent effects / Isomerization

The treatment of $[Mo_2(pyphos)_4]$ (**1**) (pyphos = 6-diphenylphosphanyl-2-pyridonate) with $[Cu(NCCH_3)_4](PF_6)$ in CH_2Cl_2 and CH_3CN mixed solvent (1:5 v/v) led to the formation of a linear tetranuclear cluster, *cis*-$[Mo_2\{Cu(NCCH_3)_2\}_2][(pyphos)_4](PF_6)_2$ (*cis*-**2a-PF₆**), as a thermodynamic product that was structurally characterized as a tetrakis[3,5-bis(trifluoromethyl)phenylborate] salt (*cis*-**2a-BArF**). In the solid-state structure of *cis*-**2a-BArF**, the Mo_2 core was bridged by two O–N chelating pyphos ligands in a *cis* fashion, in sharp contrast to a *trans* fashion in **1**. The *trans* isomer (*trans*-**2b-PF₆**) was isolated from a noncoordinating solvent such as CH_2Cl_2 and structurally characterized. The transformation from *trans*-**2b** to *cis*-**2a** proceeded in acetonitrile by means of an intramolecular rearrangement of the paddlewheel Mo_2 core upon dissolution in acetonitrile, in which the coordinating solvent stabilizes the transient, coordinatively unsaturated Mo_2 core upon the release of the pyridonate moiety from the Mo_2 core; whereas the reverse reaction did not occur under any trial conditions. A further substitution reaction at the Cu center of *cis*-**2a-PF₆** and *trans*-**2b-PF₆** with Et_4NCl afforded *cis*-**3a** and *trans*-**3b**, respectively, which have the molecular formula $[Mo_2(pyphos)_4Cu_2(Cl)_2]$. Compounds *trans*-**3a** and *cis*-**3b** do not show any solvent-dependent interconversion phenomena by changing the solvent.

Introduction

Homo- and heteromultinuclear linear transition-metal clusters linked through metal–metal bonds have attracted much interest because of their versatile chemical and physical properties within a single molecule.[1–5] Multidentate ligands with hetero donor atoms are effective platforms for the construction of multinuclear strings. In particular, the combination of soft and hard donor atoms within a multidentate ligand system has been strategically used to incorporate different kinds of metal atoms in clusters. We synthesized linear heterotetranuclear clusters by using 6-(diphenylphosphanyl)pyridin-2-olate (pyphos) as a unique bridging ligand, in which three different donor atoms (P, N, and O) serve as a suitable coordination platform to align two different kinds of transition metals in a linear manner. We previously reported the synthesis of linear heterotetranuclear clusters that bear a M···Mo–Mo···M linear array (M = second- and third-row transition elements; Rh, Ir, Pd, and Pt).[6] In these clusters, a quadruply bonded Mo^{II}_2 complex, $[Mo_2(pyphos)_4]$ (**1**)[6a,6b] is a core part of the metal string, and late-transition metals (Pd, Pt, Rh, and Ir) supported by each of two PPh_2 groups are located in axial positions of the Mo_2 core of **1** (Scheme 1). As an extension of our continuing interest in this area, we focused on the synthesis of linear heteronuclear clusters of Mo and first-row transition metals such as Cu. Herein we report the synthesis, characterization, and solvent-dependent *cis*/*trans* isomerism around the paddlewheel Mo_2 moiety.

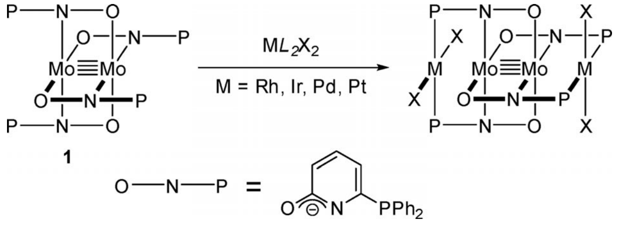

Scheme 1.

Results and Discussion

Treatment of **1** with $[Cu(NCCH_3)_4](PF_6)$ (2 equiv.) in CH_2Cl_2 at room temperature for 2 d led to the isolation of a linear tetranuclear cluster, *trans*-$[Mo_2\{Cu(CH_3CN)_2\}_2(pyphos)_4][(PF_6)_2]$ (*trans*-**2a-PF₆**) (Scheme 2). The prefix

---

[a] Department of Chemistry, Graduate School of Engineering Science, Osaka University,
Toyonaka, Osaka 560-8531, Japan
Fax: +81-6-6850-6249
E-mail: mashima@chem.es.osaka-u.ac.jp

© 2010 Wiley-VCH Verlag GmbH & Co. KGaA, Weinheim

"*trans*" stands for the *trans* orientation of pyphos coordination at the Mo_2 core. The ^1H NMR spectrum of *trans*-**2a-PF$_6$** displayed a set of signals due to the pyphos ligand together with a distinct singlet due to the coordinated CH_3CN. The $^{31}P\{^1H\}$ NMR spectrum of *trans*-**2a-PF$_6$** shows a sharp singlet at δ = 4.94 ppm, a chemical shift value that is significantly lower-field-shifted compared to that of the parent complex **1** (δ = –7.8 ppm), thus indicating the coordination of two magnetically equivalent P atoms to each Cu center (Table 1).[7]

Table 1. $^{31}P\{^1H\}$ NMR spectroscopy chemical shift data for synthesized complexes.

Complexes	δ [ppm]
1	–7.80
trans-**2a-PF$_6$**	4.94
cis-**2b-PF$_6$**	6.40
cis-**2b-BArF**	6.65
cis-**2c-BArF**	7.00
trans-**3a**	4.54
cis-**3b**[a]	–

[a] Insoluble in common organic solvents.

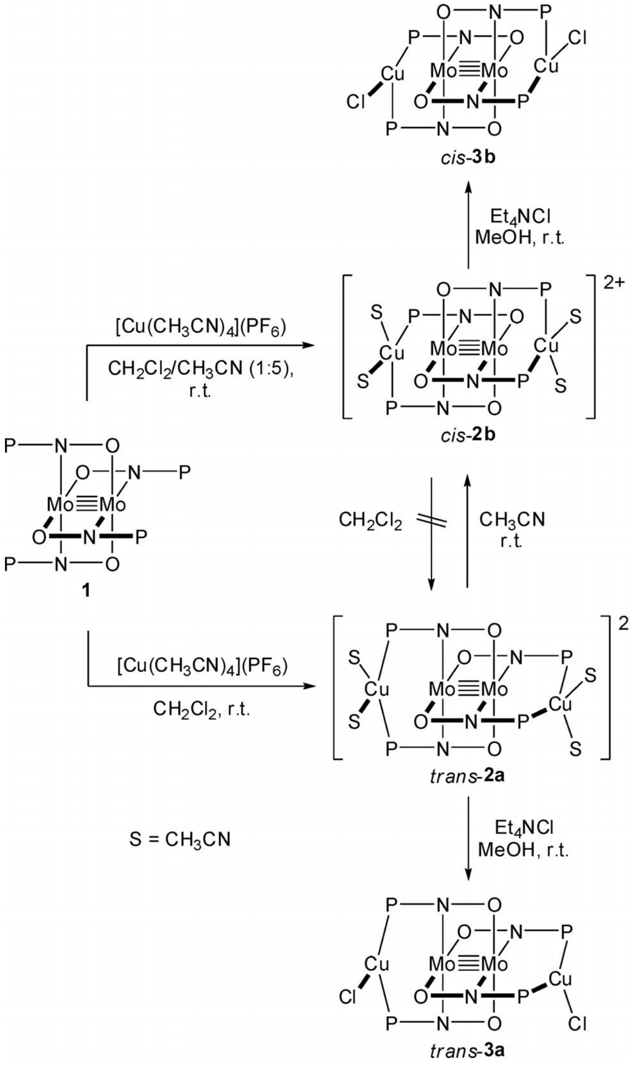

Scheme 2. Solvent-dependent synthesis of *cis*/*trans* isomerism.

The molecular structure of *trans*-**2a-PF$_6$** was analyzed by X-ray crystallography. In the solid-state structure of *trans*-**2a-PF$_6$** (Figure 1, Scheme 2), the asymmetric unit contains two PF_6 anions and one cationic linear tetranuclear cluster of Mo^{II} and Cu^{I} supported by four pyphos ligands in which the Mo_2 unit was the core part of the linear metal string and two Cu^{I} atoms were positioned at the axial position of the Mo_2 core supported by PPh_2 groups. The Mo_2 core was bridged by two O–N chelating pyphos ligands in a *trans* coordinating fashion, which is similar to the earlier reported observation (Scheme 1). Each Cu^{I} center assumed a tetrahedral geometry with two phosphorus atoms of the pyphos ligands and two nitrogen atoms of loosely bound acetonitrile molecules. The average bond lengths of Cu–P and Cu–N(acetonitrile) were 2.289(11) and 2.063(3) Å, respectively. The average P–Cu–P angle was 140.88(4)° (Table 2). This indicates that the geometry of Cu^{I} was sufficiently distorted from standard tetrahedral geometry. The Mo_2 core had a quadruple bond based on the Mo···Mo bond length of 2.106(6) Å, and, accordingly, there were no bonding interactions between the Cu and Mo atoms [Mo···Cu 3.167(2) Å].

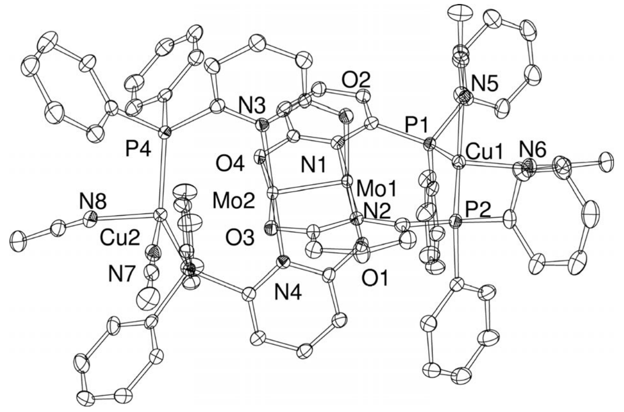

Figure 1. ORTEP view of the crystal structure of the cation of *trans*-**2a-PF$_6$** with atom numbering scheme (except carbon atoms) and 50% thermal ellipsoids. Hydrogen atoms are omitted for clarity.

In contrast to the synthesis of *trans*-**2a-PF$_6$** in CH_2Cl_2 as solvent (Scheme 2), treatment of **1** with $[Cu(NCCH_3)_4](PF_6)$ (2 equiv.) in a mixture (5:1) of acetonitrile and dichloromethane at room temperature for 2 d led to the isolation of a linear tetranuclear cluster, *cis*-$[Mo_2\{Cu(CH_3CN)_2\}_2(pyphos)_4][(PF_6)_2]$ (*cis*-**2b-PF$_6$**) (Scheme 2). The ^1H NMR spectrum of *cis*-**2b-PF$_6$** displayed a set of signals due to the pyphos ligand together with a distinct singlet due to the coordinated CH_3CN. A notable difference between *cis* and *trans* isomers was that the $^{31}P\{^1H\}$ NMR spectrum of *cis*-**2b-PF$_6$** displayed a sharp singlet at δ = 6.40 ppm, which is slightly high-field shifted relative to that of *trans*-**2a-PF$_6$** (δ = 4.94 ppm), probably due to the different geometry, *cis* or *trans*, around the Mo_2 core.

© 2010 Wiley-VCH Verlag GmbH & Co. KGaA, Weinheim

Table 2. Selected bond lengths and angles for the synthesized complexes.

	Bond lengths [Å] and angles [°]					
trans-**2a-PF$_6$**	Mo1–O1	2.063(3)	Cu1–N5	2.054(3)	Mo1–Mo2	2.1058(6)
	Mo1–O2	2.075(3)	Cu1–N6	2.086(3)	Mo1–Cu1	3.176(3)
	Mo2–O3	2.081(3)	Cu2–N7	2.030(3)	Mo2–Cu2	3.176(5)
	Mo2–O4	2.066(3)	Cu2–N8	2.104(3)	P2–Cu1–P1	142.09(4)
	Mo1–N1	2.187(3)	Cu1–P1	2.294(2)	P4–Cu2–P3	139.68(4)
	Mo1–N2	2.187(3)	Cu1–P2	2.276 (2)	Mo1–Mo2–Cu2	174.40(7)
	Mo2–N3	2.183(3)	Cu2–P3	2.301(2)	Mo2–Mo1–Cu1	178.66(6)
	Mo2–N4	2.190(3)	Cu2–P4	2.284(2)		
cis-**2b-BArF**	Mo1–O1	2.058(2)	Cu1–P1	2.2625(7)	Mo1–Mo1[a]	2.098(4)
	Mo1–O2	2.071(2)	Cu1–P2	2.2461(7)	Mo1–Cu1	3.167(5)
	Mo1–N1	2.208(2)	Cu1–N3	2.014(2)	Mo1–Mo1[a]–Cu1	175.29(5)
	Mo1–N2	2.191(2)	Cu1–N4	2.058(2)	P2–Cu1–P1	131.38(3)
cis-**2c-BArF**	Mo1–O1	2.060(3)	Cu1–O3	2.151(4)	Mo1–Mo1[a]	2.0950(10)
	Mo1–O2	2.062(3)	Cu1–O4	2.089(3)	Mo1–Cu1	3.1328(11)
	Mo1–N1	2.205(4)	Cu1–P2	2.241(2)	P1–Cu1–P2	134.80(5)
	Mo1–N2	2.196(3)	Cu1–P1	2.232(1)	Mo1–Mo1[a]–Cu1	175.02(6)
trans-**3a**	Mo2–O1	2.082(3)	Mo1–N4	2.174(3)	Mo1–Mo2	2.0974(6)
	Mo1–O2	2.076(3)	Cu1–Cl1	2.2613(13)	Mo1–Cu1	2.9571(9)
	Mo1–O3	2.062(3)	Cu2–Cl2	2.2241(12)	Mo2–Cu2	3.0026(7)
	Mo2–O4	2.071(3)	Cu1–P4	2.2713(14)	P2–Cu2–P3	129.75(9)
	Mo1–N1	2.161(3)	Cu1–P1	2.2662(11)	P4–Cu1–P1	128.11(7)
	Mo2–N2	2.159(3)	Cu2–P2	2.2823(13)	Mo1–Mo2–Cu2	164.39(13)
	Mo2–N3	2.189(3)	Cu2–P3	2.2665(12)	Mo2–Mo1–Cu1	150.41(11)
cis-**3b**	Mo1–O1	2.041(12)	Cu1–Cl1	2.213(5)	Mo1–Mo1[a]	2.091(3)
	Mo1–O2	2.045(11)	Cu1–P1	2.228(5)	Mo1–Cu1	3.037(3)
	Mo1–N1	2.189(13)	Cu1–P2	2.219(5)	P2–Cu1–P1	125.58(19)
	Mo1–N2	2.178(13)			Mo1–Mo1[a]–Cu1	176.19(5)

[a] Symmetry-equivalent elements.

The molecular structure of *cis*-**2b** was established by X-ray analysis. Despite several attempts, we were unable to obtain suitable X-ray-quality crystals of *cis*-**2a-PF$_6$**. A metathesis reaction, however, afforded *cis*-[Mo$_2${Cu(CH$_3$CN)$_2$}$_2$(pyphos)$_4$][(BArF)$_2$] (*cis*-**2b-BArF**) (BArF = tetrakis[3,5-bis(trifluoromethyl)phenylborate]), which showed identical ^{1}H (an additional signal of BArF) and ^{31}P{^{1}H} NMR spectral features. X-ray analysis (Figure 2) of *cis*-**2b-BArF** revealed that the cationic linear tetranuclear Mo/Cu cluster has similar structural features. The only difference was found at the coordination motifs of the pyphos ligand at the Mo$_2$ core. The Mo$_2$ core was bridged by two O–N chelating pyphos ligands in a *cis* coordinating fashion, in sharp contrast to a *trans* fashion in the starting complex **1**. A similar *cis*-coordination mode of the pyphos ligand to the paddlewheel Cr$_2$ core was observed in [Cr$_2$Pt$_2$(pyphos)$_4$(Me)$_4$], in which Cr$_2$ is a core part of the tetranuclear metal string.[8] Thus, during the course of the reaction, an intramolecular rearrangement proceeded by maintaining the coordination of phosphane moieties of pyphos ligands to Cu^I atoms. Each Cu^I center possesses a tetrahedral geometry with two phosphorous atoms of the pyphos ligands and two nitrogen atoms of acetonitrile molecules. The Mo$_2$ core had a quadruple bond with an Mo···Mo bond length of 2.099(6) Å, and there were no bonding interactions between the Cu and Mo atoms [Mo···Cu 3.167(2) Å], which was a similar observation to that of *trans*-**2a-PF$_6$**. The average bond lengths of Cu–P and Cu–N(acetonitrile) were 2.245(2) and 2.050(3) Å, respectively. However, the average P–Cu–P angle was 131.88(3)°, which is expected for tetrahedral geometry.

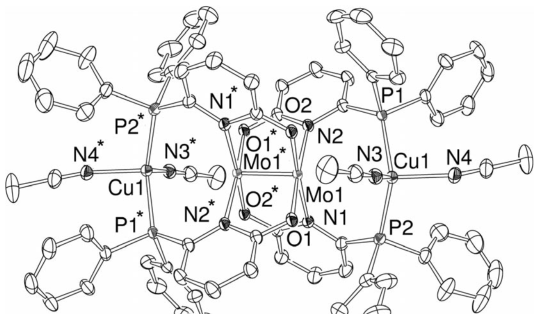

Figure 2. ORTEP view of the crystal structure of cation of *cis*-**2b-BArF** with atom numbering scheme (except carbon atoms) and 50% thermal ellipsoids. Hydrogen atoms are omitted for clarity. The asterisk stands for symmetry equivalent.

The coordinated solvent molecules at the Cu^I centers for *trans*-**2a** and *cis*-**2b** were loosely bound, as it could be reversibly exchanged between acetonitrile and DMF. When *cis*-**2b-BArF** was dissolved in a mixture of DMF and EtOH, *cis*-[Mo$_2${Cu(DMF)$_2$}$_4$(pyphos)$_4$](BArF)$_2$ (*cis*-**2c-BArF**) was obtained, and vice versa. The ^{1}H and ^{31}P{^{1}H} NMR spectra of *cis*-**2c-BArF** displayed identical signals to those of *cis*-**2a-BArF** along with an additional set of signals due to DMF. The geometry around the Cu···Mo–Mo···Cu unit of *cis*-**2c-BArF** is superimposed over that of *cis*-**2b-BArF** except for the coordination of DMF at the Cu center in *cis*-**2b-BArF**. An ORTEP view of the cation of *cis*-**2c-BArF** is

© 2010 Wiley-VCH Verlag GmbH & Co. KGaA, Weinheim

shown in Figure 3. The average bond lengths of Cu–P and Cu–O(DMF) were 2.237(2) and 2.112(5) Å, respectively, which are similar to that of *trans*-**2a-PF$_6$**. The average P–Cu–P angle was 134.81(4)°.

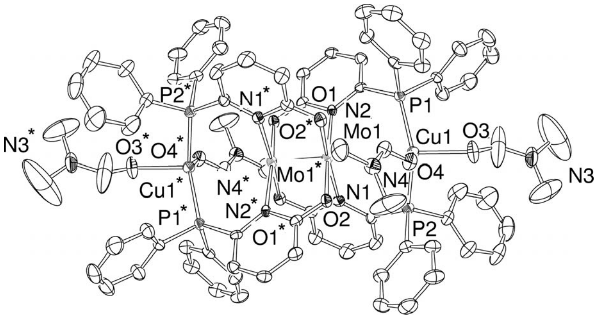

Figure 3. Crystal structure of the cation of *cis*-[$Mo_2\{Cu(DMF)_2\}_2(pyphos)_4$][$(BArF)_2$] (*cis*-**2c-BArF**) with atom numbering scheme (except carbon atoms) and 50% thermal ellipsoids. Hydrogen atoms are omitted for clarity. The asterisk stands for symmetry equivalent.

The $^{31}P\{^1H\}$ NMR spectrum of *trans*-**2a-PF$_6$** in acetonitrile as solvent displayed a sharp singlet at δ = 6.40 ppm, which is a positive shift from that in CH_2Cl_2 as solvent. The ^1H NMR spectrum of *trans*-**2a-PF$_6$** showed similar spectral features to those of *cis*-**2a-PF$_6$**. The recrystallization of *trans*-**2a-PF$_6$** from acetonitrile/ether as solvent in the presence of BArF yielded *cis*-**2b-BArF**. This indicates that the transformation from *trans*-**2b** to *cis*-**2b** proceeded in acetonitrile, whereas the reverse reaction did not occur under any trial conditions (Scheme 2). This conversion was very fast and could not be monitored, even when using $^{31}P\{^1H\}$ NMR spectral analysis, which restricts our efforts to analyze the nature of such *cis*/*trans* isomerism. Thus, it is clear that *trans*-**2a** isolated from dichloromethane is a kinetic product, whereas *cis*-**2b** from acetonitrile is a thermodynamic product. The relative thermodynamic stability of *cis*-**2b** over *trans*-**2a** can be accounted for by the structural feature that *trans*-**2a** is strained around each Cu^I center: the Cu–P bond length in the *trans* geometry is significantly longer than that of the *cis* isomer, and the P–Cu–P angle of *trans*-**2a** (140.88°) is sufficiently deviated from the tetrahedral relative to that of *cis*-**2b** (131.83°). The intramolecular rearrangement occurred in one direction from a *trans*-to-*cis* conversion. The role of the coordinating solvent in this isomerization is that acetonitrile stabilizes the transient, coordinatively unsaturated Mo_2 core upon the release of the pyridonate moiety from the Mo_2 core, as observed for $[Mo_2(CH_3CN)_{10}]^{4+}$ and $[Mo_2(OCOR)_2(CH_3CN)_6]^{2+}$.[9]

We attempted a substitution reaction at the Cu center without disturbing the geometry around the Mo_2 core (Scheme 2). The addition of a methanolic solution of Et_4NCl into the dichloromethane solution of *trans*-**2a-PF$_6$** precipitated *trans*-[$Mo_2(CuCl)_2(pyphos)_4$] (*trans*-**3a**), the $\{^1H\}$ NMR spectrum of which was very similar to *trans*-**2a-PF$_6$**; the $^{31}P\{^1H\}$ NMR spectrum showed one sharp singlet at δ = 4.54 ppm, thereby suggesting the same geometry around the Mo_2 core as that of *trans*-**2a-PF$_6$**. In contrast, the addition of a methanolic solution of Et_4NCl to an acetonitrile solution of *cis*-**2b-PF$_6$** yielded *cis*-**3b**, the low solubility of which in organic solvents hampered further characterization.

The crystal structures of *trans*-**3a** and *cis*-**3b** were determined by X-ray analyses (Figure 4). The Figure 4 shows that the Cu^I centers of both *trans*-**3a** and *cis*-**3b** adopted trigonal planer geometry with two phosphorus atoms and one chloride ion [average Cu–Cl 2.224(2) Å]. There was a significant difference in the Mo_2 core of *cis*-**3a** and *trans*-**3b**. For *trans*-**3a**, the Mo_2 core was bridged by two O–N chelating pyphos ligands in *trans* fashion with an quite elongated average Cu–P bond [2.271(2) Å] and P–Cu–P angle was 127.75(5)°. For *cis*-**3b**, the coordination geometry of the pyphos ligand at the Mo_2 core was in *cis* fashion with a Cu–P bond length and P–Cu–P angle of 2.223(5) Å and 125.56(5)°. The geometrical parameters at Cu centers of *cis*/*trans*-**3** is well agreement with the reported stable [$Cu(PPh_3)_2Cl$] complex. This results indicates the more stability around the Cu center of *trans*-**3a** and *cis*-**3b** complexes over the *trans*-**2a-PF$_6$** and *cis*-**2b-PF$_6$**. It is interesting to note that, *trans*-**3a** and *cis*-**3b** does not show any solvent dependent inter conversion phenomena by changing the solvent.

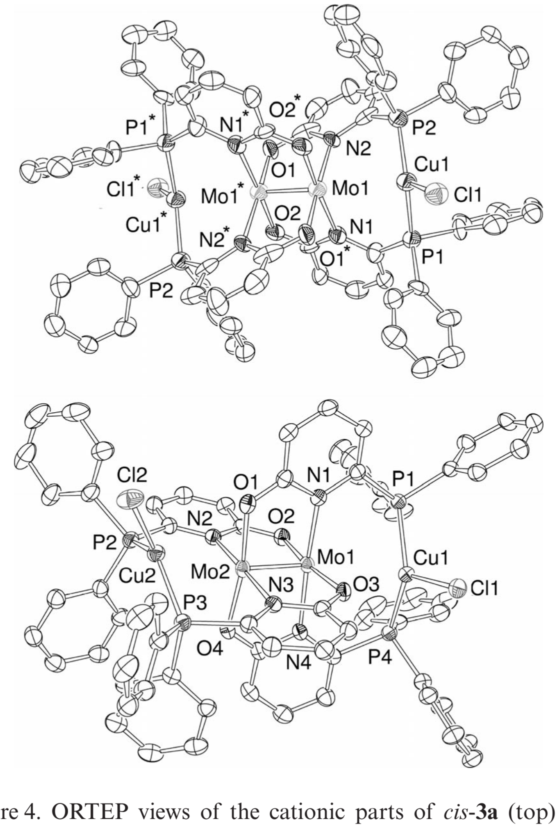

Figure 4. ORTEP views of the cationic parts of *cis*-**3a** (top) and *trans*-**3b** (bottom) with atom numbering scheme (except carbon atoms) and 50% thermal ellipsoids. Hydrogen atoms are omitted for clarity. The asterisk stands for symmetry equivalent.

Conclusions

In summary, we demonstrate the synthesis and characterization of a set of *cis* and *trans* forms of linear tetranuclear clusters of $[Mo_2\{Cu(CH_3CN)_2\}_2(pyphos)_4]^{2+}$ and $[Mo_2(CuCl)_2(pyphos)_4]$. Unlike earlier reports of late transition metals,[7] Cu^I, a first-row transition metal, preferred a *cis* geometry around the paddlewheel Mo_2 core as a thermodynamic product. The *trans* isomer isolated from a noncoordinating solvent was a kinetic product of the reaction of **1** and Cu^I, and, accordingly, it irreversibly turned into the *cis* isomer in acetonitrile. Such interconversion was not observed for the corresponding chloro derivative.

Experimental Section

Materials and Physical Methods: All manipulations for air- and moisture-sensitive compounds were carried out using standard Schlenk techniques under an argon atmosphere. Solvents were distilled under an atmosphere of argon with sodium benzophenone ketyl (diethyl ether and hexane) and P_2O_5 (CH_2Cl_2 and CD_3CN), respectively. Acetonitrile was degassed and stored over activated molecular sieves (MS, 3 Å) under an atmosphere of argon and CD_2Cl_2 was degassed and stored over activated MS 4 Å under an argon atmosphere. Other reagents purchased from commercial sources were used without further purification. 6-Diphenylphosphanyl-2-pyridone (pyphosH) and $[Mo_2(pyphos)_4]$ were prepared[6] according to the literature methods. $[Cu(CH_3CN)_4]PF_6$, Et_4NCl, and $Na[B\{3,5\text{-}(CF_3)_2C_6H_3\}_4]$ (**NaBArF**) were obtained from _Aldrich. Solvents were distilled and dried by standard procedure. ^1H and ^{31}P NMR (400 MHz) spectra were measured with a Bruker Avance III-400 spectrometer. Elemental analyses were performed with a Perkin–Elmer 2400 microanalyzer. All were recorded at 35 °C unless mentioned otherwise. ^1H NMR spectra were referenced to an internal solvent and corrected to TMS. $^{31}P\{^1H\}$ NMR spectra were referenced to an external reference of 85% H_3PO_4 at ($\delta = 0.00$ ppm).

X-ray Structure Determination: Suitable diffraction-quality crystals were obtained from the crystallization procedures described in the synthesis. In each case, a crystal of suitable dimensions was mounted on a CryoLoop (Hampton Research Corp.) with a layer of light mineral oil and placed in a nitrogen stream at 120(2) K. All measurements were made with a Rigaku RAXIS RAPID imaging plate area detector with graphite-monochromated Mo-K_α (λ = 0.71075 Å) radiation. Cell constants and orientation matrix for data collection, obtained from least-squares refinement by using the setting angles of 11 carefully centered reflections in the range $29.54 < 2\theta < 29.97°$ corresponded to a primitive triclinic cell with dimensions listed in Table 2, in which details of the data collection were summarized. The weak reflections $[I < 10.0\sigma(I)]$ were rescanned (maximum of 5 scans) and the counts were accumulated to ensure good counting statistics. Stationary background counts were recorded on each side of the reflection. The ratio of peak counting time to background counting time was 2:1. The diameter of the incident beam collimator was 1.0 mm, the crystal-to-detector distance was 235 mm, and the computer-controlled detector aperture was set to 3.0 × 3.5 mm (horizontal × vertical). The intensities of three representative reflections were measured after every 150 reflections. An empirical absorption correction based on azimuthal scans of several reflections was applied, which resulted in transmission factors that ranged from 0.70 to 0.98. The data were corrected for Lorentz and polarization effects. The space group of this compound was determined based on the lack of systematic absence and intensity statistics. The structure was solved using SIR97[10] and refined using SHELXL-97.[11] Full-matrix least-squares/difference Fourier cycles were performed; these located the remaining non-hydrogen atoms. All non-hydrogen atoms were refined with anisotropic displacement parameters.

For *cis*-**2c-BArF**, one coordinated DMF molecule in an anionic Mo–Cu cluster and one CF_3 group of counteranion tetrakis[3,5-bis(trifluoromethyl)phenylborate] were disordered over two positions. For *cis*-**2b-BArF**, four CF_3 groups of counteranion tetrakis[3,5-bis(trifluoromethyl)phenylborate] were disordered over two positions. Those disorder groups were refined with free part instruction using SHELXL-97.

Table 3. Crystallographic data for synthesized complexes.

Complex	*trans*-**2a-PF$_6$**	*cis*-**2b-BArF**	*cis*-**2c-BArF**	*trans*-**3a**	*cis*-**3b**
Empirical formula	$C_{84}H_{76}Cu_2F_{12}$-$Mo_2N_{12}O_4P_6$	$C_{144}H_{90}B_2Cl_8Cu_2F_{48}$-$Mo_2N_8O_4P_4$	$C_{144}H_{104}B_2Cu_2F_{48}$-$Mo_2N_8O_8P_4$	$C_{71}H_{58}Cl_8Cu_2$-$Mo_2N_4O_4P_4$	$C_{74}H_{64}Cl_{14}Cu_2$-$Mo_2N_4O_4P_4$
Formula weight	2050.37	3656.32	3450.83	1757.68	2012.45
Crystal system	monoclinic	triclinic	triclinic	monoclinic	monoclinic
Space group	$P2_1/n$	$P\bar{1}$	$P\bar{1}$	$P2_1/c$	$P2_1/c$
T [K]	100	100	100	100	100
Z	4	1	1	4	2
a [Å]	19.321(5)	13.361 (5)	14.224(5)	10.686(5)	12.866(5)
b [Å]	24.512(5)	17.242 (5)	17.022(5)	27.031(5)	21.596(5)
c [Å]	19.911(5)	17.968 (5)	17.188(5)	24.709(5)	15.818(4)
α [°]	90	73.64 (5)	62.418(5)	90	90
β [°]	114.358(5)	74.10 (5)	80.713(5)	94.398(5)	113.18(2)
γ [°]	90	88.90 (5)	80.201(5)	90	90
V [Å^3]	8590(4)	3812.3 (3)	3619(2)	7116(4)	4040(2)
$D_{calcd.}$ [g m^{-3}]	1.586	1.593	1.583	1.641	1.654
F(000)	4144	1822	1732	3528	2016
Absorption [mm^{-1}]	0.969	0.732	0.625	1.376	1.413
θ range [°]	3.04–27.44	3.00–30.45	2.99–30.45	3.01–30.50	3.16–27.48
Collected reflections	87967	78098	70034	117004	59318
Unique reflections	17823	23143	22004	21729	9268
GOF [F^2]	0.972	1.039	1.009	1.042	1.056
R_1[a] (wR_2)[b] [%]	0.0483 (0.1231)	0.0497 (0.1388)	0.0867 (0.1354)	0.0632 (0.1419)	0.0746 (0.2453)

[a] $R_1 = \Sigma||F_o| - |F_c||/\Sigma|F_o|$. [b] $wR_2 = \{\Sigma[w(F_o^2 - F_c^2)^2]/\Sigma[w(F_o^2)^2]\}^{1/2}$.

All hydrogen atoms were included in the refinement on calculated positions riding on their carrier atoms (C_{sp^2}–H = 0.93 Å, U_{iso}(H) = 1.2U_{eq}(C) Å^2, C_{sp^3}–H(methylene) = 0.97 Å, U_{iso}(H) = 1.2U_{eq}(C) Å^2, C_{sp^3}–H(methyl) = 0.96 Å, U_{iso}(H) = 1.5U_{eq}(C) Å^2). The function minimized was $[\Sigma w(F_o^2 - F_c^2)^2]$ ($w = 1/[\sigma^2(F_o^2) + (0.1061P)^2 + 0.0000P]$), in which $P = [\max(F_o^2,0) + 2F_o^2]/3$ with $\sigma^2(F_o^2)$ from counting statistics. The functions $R1$ and $wR2$ were $(\Sigma||F_o| - |F_c||)/\Sigma|F_o|$ and $[\Sigma w(F_o^2 - F_c^2)^2/\Sigma(wF_o^4)]^{1/2}$, respectively. Crystal structures were viewed using ORTEP.[12] Selected crystallographic data parameters are listed in Table 3.

CCDC-787922 (for *cis*-**2b-BArF**), -787923 (for *cis*-**2c-BArF**), -787924 (for *cis*-**3b**), -787925 (for *trans*-**2a-PF$_6$**), and -787926 (for *trans*-**3a**) contain the supplementary crystallographic data for this paper. These data can be obtained free of charge from The Cambridge Crystallographic Data Center via www.ccdc.cam.ac.uk/data_request/cif.

Syntheses: All procedures were carried out by using standard Schlenk techniques under argon.

***cis*-[Mo$_2${Cu(CH$_3$CN)$_2$}$_2$(pyphos)$_4$][(PF$_6$)$_2$] (*cis*-2b-PF$_6$):** A solution of [Cu(CH$_3$CN)]PF$_6$ (37 mg, 0.1 mmol) in acetonitrile (5 mL) was mixed with a solution of compound **1** (65 mg, 0.05 mmol) in dichloromethane (1 mL). The reaction mixture was stirred for 2 d at room temperature. Then the solution was filtered and the solvent was removed under vacuum to get a red solid residue of *cis*-**2b-PF$_6$**. It was washed with ethanol/diethyl ether and dried under vacuum. The yield was 72% (68 mg) based on product formation. ^{1}H NMR (400 MHz, CD$_3$CN, 30 °C): δ = 2.11 (s, 12 H, 4CuNCCH$_3$), 6.47–6.50 (m, 8 H), 7.21–7.25 (m, 16 H), 7.35–7.42 (m, 20 H), 7.52 (m, 8 H) ppm. ^{31}P{^{1}H} NMR (400 MHz, CD$_3$CN, 30 °C): δ = 6.34 (s) ppm. $C_{76}H_{64}Cu_2F_{12}Mo_2N_8O_4P_6$ (1884.04): calcd. C 48.40, H 3.42, N 5.94; found C 48.12, H 3.49, N 5.76.

***cis*-[Mo$_2${Cu(CH$_3$CN)$_2$}$_2$(pyphos)$_4$][(BArF)$_2$]·2CH$_2$Cl$_2$ (*cis*-2b-BArF):** A solution of NaBArF (89 mg, 0.1 mmol) in MeOH (5 mL) was mixed with a solution of *cis*-**2b-PF$_6$** (99 mg, 0.05 mmol) in CH$_3$CN (5 mL). The reaction mixture was stirred for 1 h at room temperature. Then the reaction mixture was filtered, and the solvent was removed under vacuum to obtain *cis*-**2b-BArF** as a red solid mass. It was washed with ethanol followed by diethyl ether and dried under vacuo. Diffraction-quality crystals were obtained by slow diffusion of methanol (5 mL) at room temperature into the solution of *cis*-**2b-BArF** in a mixture of solvents [dichloromethane (2 mL) and acetonitrile (0.5 mL)] to give red crystals of *cis*-**2b-BArF·2CH$_2$Cl$_2$**. The yield of the crystals was 68% (124.2 mg) based on expected product formation. ^{1}H NMR (400 MHz, CD$_3$CN, 30 °C): δ = 2.09 (s, 12 H, CuNCCH$_3$), 6.22 (d, $^3J_{H,H}$ = 8.4 Hz, 4 H), 6.52 (d, $^3J_{H,H}$ = 6.4 Hz, 4 H), 6.98 (dd, $^3J_{H,H}$ = 6.8 Hz, 8 H), 7.27–7.59 (m, 40 H), 7.66 (br. s, 16 H, BArF), 7.70 (s, 8 H, BArF) ppm. ^{31}P{^{1}H} NMR (400 MHz, CD$_3$CN, 30 °C): δ = 6.65 (s) ppm. $C_{144}H_{90}B_2Cl_8Cu_2F_{48}Mo_2N_8O_4P_4$ (3656.3): calcd. C 47.28, H 2.48, N 3.06; found C 47.32, H 2.44, N 2.97.

***trans*-[Mo$_2${Cu(CH$_3$CN)$_2$}$_2$(pyphos)$_4$][(PF$_6$)$_2$]·2CH$_3$CN (*trans*-2a-PF$_6$):** A solution of [Cu(CH$_3$CN)]PF$_6$ (37 mg, 0.1 mmol) in dichloromethane (2 mL) was mixed with a solution of compound **1** (65 mg, 0.05 mmol) in dichloromethane (2 mL). The reaction mixture was stirred for 2 d. Then the reaction mixture was filtered and EtOH (10 mL) was layered onto the filtrate. After several days, fine red crystals of *trans*-**2a-PF$_6$** were obtained, which were filtered, washed with ethanol/diethyl ether and dried under a flow of argon. The yield of the crystals was 79% (80.9 mg) based on expected product formation. Diffraction-quality crystals were obtained by slow diffusion of ethanol at room temperature into the solution of *trans*-**2a-PF$_6$** in dichloromethane and a few drops of acetonitrile. ^{1}H NMR (400 MHz, CD$_2$Cl$_2$, 30 °C): δ = 1.98 (s, 12 H, CuNCCH$_3$), 6.51 (br. s, 4 H), 6.68 (br. s, 4 H), 7.18 (m, 16 H), 7.34–7.37 (m, 16 H), 7.48–7.51 (m, 16 H) ppm. ^{31}P{^{1}H} NMR (400 MHz, CD$_2$Cl$_2$, 30 °C): δ = 4.94 (s) ppm. $C_{84}H_{76}Cu_2F_{12}Mo_2N_{12}O_4P_6$ (2050.37): calcd. C 49.21, H 3.74, N 8.20; found C 49.19, H 3.76, N 8.23.

***cis*-[Mo$_2${Cu(DMF)$_2$}$_2$(pyphos)$_4$][(BArF)$_2$] (*cis*-2c-BArF):** Compound *cis*-**2b-BArF** (37 mg, 0.01 mmol) was dissolved in DMF (1 mL). The solution was stirred at 80 °C for 12 h. Slow diffusion of ethanol (8 mL) at room temperature into the reaction mixture yielded red crystals of *cis*-**2c-BArF**. Crystals were separated by filtration, washed with ethanol/diethyl ether, and dried under vacuum. The yield of the crystals was 82% (28.3 mg) based on the expected product formation. Diffraction-quality crystals were obtained by slow diffusion of ethanol at room temperature into the solution of ***cis*-2c-BArF** in DMF. ^{1}H NMR (400 MHz, CD$_2$Cl$_2$, 30 °C): δ = 2.74 (d, $J_{H,H}$ = 9.6 Hz, 24 H, DMF), 6.04 (d, $^3J_{H,H}$ = 8.8 Hz, 4 H), 6.56 (d, $^3J_{H,H}$ = 6.4 Hz, 4 H), 7.06 (m, 8 H), 7.16 (m, 8 H), 7.29 (m, 8 H), 7.44 (m, 16 H), 7.52 (br. s, 16 H, 2BArF), 7.57 (m, 8 H), 7.70 (s, 8 H, 2BArF) ppm. ^{31}P{^{1}H} NMR (400 MHz, CD$_2$Cl$_2$, 30 °C): δ = 7.00 (s) ppm. $C_{144}H_{104}B_2Cu_2F_{48}Mo_2N_8O_8P_4$ (3450.83): calcd. C 50.09, H 3.04, N 3.25; found C 49.88, H 3.15, N 3.06.

***trans*-[Mo$_2$(CuCl)$_2$(pyphos)$_4$]·3CH$_2$Cl$_2$ (*trans*-3a):** A solution of Et$_4$NCl (35 mg, 0.2 mmol) in methanol (10 mL) was layered with a solution of *trans*-**2a-PF$_6$** (94 mg, 0.05 mmol) in dichloromethane (2 mL) in a 40 mL Schlenk tube at room temperature. The platelike red crystals of **3a** were obtained after 2 d; they were isolated by filtration, washed with methanol/diethyl ether, and dried under a flow of argon. The yield of the crystals was 79% (69.43 mg) based on expected product formation. Diffraction-quality crystals were obtained by slow diffusion of hexane at room temperature into the solution of ***cis*-2c-BArF** in dichloromethane. ^{1}H NMR (400 MHz, CD$_2$Cl$_2$, 30 °C): δ = 6.34 (d, $^3J_{H,H}$ = 6.8 Hz, 4 H), 6.57 (d, $^3J_{H,H}$ = 8.5 Hz, 4 H), 7.22–7.32 (m, 36 H), 7.39–7.42 (m, 8 H) ppm. ^{31}P{^{1}H} NMR (400 MHz, CD$_2$Cl$_2$, 30 °C): δ = 4.54 (s) ppm. $C_{71}H_{58}Cl_8Cu_2Mo_2N_4O_4P_4$ (1757.68): calcd. C 48.49, H 3.33, N 3.19; found C 48.36, H 3.25, N 3.11.

***cis*-[Mo$_2$(CuCl)$_2$(pyphos)$_4$]·6CH$_2$Cl$_2$ (*cis*-3b):** A solution of Et$_4$NCl (35 mg, 0.2 mmol) in methanol (20 mL) was layered with a solution of *cis*-**2b-BArF** (185 mg, 0.05 mmol) in acetonitrile (2 mL) in a 40 mL Schlenk tube at room temperature. The needle-shaped red crystals of **3b** were obtained after 2 d; they were isolated by filtration, washed with methanol/diethyl ether, and dried under a flow of argon. The yield of the crystals was 88% (88.56 mg) based on expected product formation. This compound was not soluble in common organic solvent, which restricted the NMR spectroscopic studies. $C_{74}H_{64}Cl_{14}Cu_2Mo_2N_4O_4P_4$ (2012.45): calcd. C 44.14, H 3.21, N 2.78; found C 43.89, H 3.19, N 2.97.

Acknowledgments

K. P. acknowledges financial support from the Japan Society for the Promotion of Science (JSPS) fellowship and the Grant-in-Aid for Scientific Research provided by the JSPS. This work is financially supported by a Grant-in-Aid from the Ministry of Education, Culture, Sports, Science and Technology of Japan.

---

[1] F. A. Cotton, C. A. Murio, R. A. Walton, *Multiple Bonds Between Metal Atoms*, 3rd ed., Springer Science and Business Media, Oxford, **2005**.

[2] P. Braunstein, L. A. Oro, P. R. Raithby, *Metal Cluster in Chemistry*, Wiley-VCH, Weinheim, **1999**, vol. 1–3.

[3] a) F. A. Cotton, C. Lin, C. A. Murillo, *Acc. Chem. Res.* **2001**, *34*, 759; b) M. H. Chisholm, *Acc. Chem. Res.* **2000**, *33*, 53; c) M. H. Chisholm, N. J. Patmore, *Acc. Chem. Res.* **2007**, *40*, 19; d) M. H. Chisholm, A. M. Macintosh, *Chem. Rev.* **2005**, *105*, 2949; e) K. Mashima, *Bull. Chem. Soc. Jpn.* **2010**, *83*, 299–312.

[4] For leading references on homoleptic linear clusters, see: a) J. K. Bera, K. R. Dunbar, *Angew. Chem. Int. Ed.* **2002**, *41*, 4453; b) I.-W. P. Chen, M.-W. Fu, W.-H. Tseng, J.-Y. Yu, S.-H. Wu, C.-J. Ku, C.-H. Chen, S.-H. Peng, *Angew. Chem. Int. Ed.* **2006**, *45*, 5814–5818; c) M. Bénard, J. F. Berry, F. A. Cotton, C. Gaudin, X. López, C. A. Murillo, M.-M. Rohmer, *Inorg. Chem.* **2006**, *45*, 3932; d) X. López, M.-Y. Huang, G.-C. Huang, S.-M. Peng, F.-Y. Li, M. Bénard, M.-M. Rohmer, *Inorg. Chem.* **2006**, *45*, 9075; e) I. P.-C. Liu, M. Benard, H. Hasanov, I.-W. P. Chen, W.-H. Tseng, M.-D. Fu, M.-M. Rohmer, C.-H. Chen, G.-H. Lee, S.-H. Peng, *Chem. Eur. J.* **2007**, *13*, 8667–8677; f) W.-Z. Wang, R. H. Ismayilov, G.-H. Lee, I. P.-C. Liu, C.-Y. Yeh, S.-M. Peng, *Dalton Trans.* **2007**, 830–839; g) C. Yin, G.-C. Huang, C.-K. Kuo, M.-D. Fu, H.-C. Lu, J.-H. Ke, K.-N. Shih, Y.-L. Huang, G.-H. Lee, C.-Y. Yeh, C.-h. Chen, S.-M. Peng, *J. Am. Chem. Soc.* **2008**, *130*, 10090–10092; h) Y. Tatsumi, T. Murahashi, M. Okada, S. Ogoshi, H. Kurosawa, *Chem. Commun.* **2008**, 477; i) T.-T. Luo, H.-C. Wu, Y.-C. Jao, S.-M. Huang, T.-W. Tseng, Y.-S. Wen, G.-H. Lee, S.-M. Peng, K.-L. Lu, *Angew. Chem. Int. Ed.* **2009**, *48*, 9461–9464.

[5] For leading references on heteroleptic linear clusters, see: a) R. Clérac, F. A. Cotton, K. R. Dunbar, C. A. Murillo, X. Wang, *Inorg. Chem.* **2001**, *40*, 420; b) T. Yamaguchi, F. Yamazaki, T. Ito, *J. Am. Chem. Soc.* **2001**, *123*, 743; c) E. Goto, R. A. Begum, S. Zhan, T. Tanase, K. Tanigaki, K. Sakai, *Angew. Chem. Int. Ed.* **2004**, *43*, 5029; d) J. F. Berry, F. A. Cotton, C. A. Murillo, *Organometallics* **2004**, *23*, 2503; e) C.-K. Kuo, J.-C. Chang, C.-Y. Yeh, G.-H. Lee, C.-C. Wang, S.-M. Peng, *Dalton Trans.* **2005**, 3696; f) T. Murahashi, R. Inoue, K. Usui, S. Ogoshi, *J. Am. Chem. Soc.* **2009**, *131*, 9888.

[6] a) K. Mashima, H. Nakano, A. Nakamura, *J. Am. Chem. Soc.* **1993**, *115*, 11632–11633; b) K. Mashima, H. Nakano, A. Nakamura, *J. Am. Chem. Soc.* **1996**, *118*, 9083–9095; c) H. Nakano, A. Nakamura, K. Mashima, *Inorg. Chem.* **1996**, *35*, 4007–4012; d) K. Mashima, A. Fukumoto, H. Nakano, Y. Kaneda, K. Tani, A. Nakamura, *J. Am. Chem. Soc.* **1998**, *120*, 12151–12152; e) T. Ruffer, M. Ohashi, A. Shima, H. Mizomoto, Y. Kaneda, K. Mashima, *J. Am. Chem. Soc.* **2004**, *126*, 12244–12245; f) K. Mashima, Y. Shimoyama, Y. Kusumi, A. Fukumoto, T. Yamagata, M. Ohashi, *Eur. J. Inorg. Chem.* **2007**, 235–238; g) M. Ohashi, A. Shima, T. Ruffer, H. Mizomoto, Y. Kaneda, K. Mashima, *Inorg. Chem.* **2007**, *46*, 6702–6714; h) K. Mashima, A. Shima, K. Nakao, A. Fukumoto, Y. Kaneda, Y. Kusumi, *Inorg. Chem.* **2009**, *48*, 1879–1886.

[7] The single resonance in the $^{31}P\{^1H\}$ NMR spectrum of *cis*-**2a-(PF$_6$)$_2$** (δ = 6.34 ppm) is almost equal to that of [Cu$_3$(pyphos)$_4$]ClO$_4$ [δ = 7.44 (s)]; a) T. Krauter, B. Neumuller, *Polyhedron* **1996**, *15*, 2851–2857; b) S. Parsons, Z. Pikramenou, G. A. R. E. Solan, P. Winpenny, *J. Cluster Sci.* **2000**, *11*, 227–232.

[8] a) K. Mashima, M. Tanaka, K. Tani, A. Nakamura, W. Mori, S. Takeda, K. Yamaguchi, *J. Am. Chem. Soc.* **1997**, *119*, 4307–4308; b) M. Tanaka, K. Mashima, M. Nishino, S. Takeda, W. Mori, K. Tani, K. Yamaguchi, A. Nakamura, *Bull. Chem. Soc. Jpn.* **2001**, *74*, 67–75.

[9] a) F. A. Cotton, A. H. Reid, W. Schwotzer Jr., *Inorg. Chem.* **1985**, *24*, 3965–3968; b) F. A. Cotton, K. J. Wiesinger, *Inorg. Synth.* **1992**, *29*, 134–137.

[10] A. Altomare, M. C. Burla, M. Camalli, G. L. Cascarano, C. Giacovazzo, A. Guagliardi, A. G. G. Moliterni, G. Polidori, R. Spagna, *J. Appl. Crystallogr.* **1999**, *32*, 115–119.

[11] G. M. Sheldrick, *SHELX97: A Program for Crystal Structure Analysis* (rel. 97-2), University of Göttingen, Germany, **1997**.

[12] L. J. Farrugia, *J. Appl. Crystallogr.* **1997**, *30*, 565.

Received: August 23, 2010
Published Online: November 22, 2010

© 2010 Wiley-VCH Verlag GmbH & Co. KGaA, Weinheim